

Erdheim-Chester disease: look it in the eye.

An orbital magnetic resonance imaging study

Julien Haroche,^{1*} Yoram Gueniche,^{2*} Damien Galanaud,³ Fleur Cohen-Aubart,¹ Didier Dormont,³ Theophile Rousseau,⁴ Zahir Amoura,¹ Valerie Touitou,⁴ and Natalia Shor^{2,5}

¹Sorbonne Université, Assistance Publique-Hôpitaux de Paris, Service de Médecine Interne 2, Centre National de Référence des Histiocytoses, Hôpital Pitié-Salpêtrière; ²Assistance Publique-Hôpitaux de Paris, Service de Neuroradiologie; ³Sorbonne université, Assistance Publique-Hôpitaux de Paris, Service de Neuroradiologie; ⁴Sorbonne Université, Assistance Publique-Hôpitaux de Paris, Service d'Ophtalmologie and ⁵Service de Neuroimagerie, Centre Hospitalier National d'Ophtalmologie des Quinze-Vingts, Paris, France

*JH and YG contributed equally as co-first authors.

Correspondence: N. Shor
natalia.shor@aphp.fr

J. Haroche
julien.haroche@aphp.fr

Received: December 14, 2021.

Accepted: April 12, 2022.

Prepublished: April 28, 2022.

<https://doi.org/10.3324/haematol.2021.280510>

©2022 Ferrata Storti Foundation

Published under a CC-BY-NC license



Abstract

Erdheim-Chester disease (ECD) is a rare L-group histiocytosis. Orbital involvement is found in a third of cases, but few data are available concerning the radiological features of ECD-related orbital disease (ECD-ROD). Our aim was to characterize the initial radiological phenotype and outcome of patients with ECD-ROD. Initial and follow-up orbital magnetic resonance imaging (MRI) from the patients with histologically proven ECD at a national reference center were reviewed. Pathological orbital findings were recorded for 45 (33%) of the 137 patients included, with bilateral involvement in 38/45 (84%) cases. The mean age (\pm standard deviation) of these patients was 60 (\pm 11.3) years and 78% were men. Intraconal fat infiltration around the optic nerve sheath adjacent to the eye globe (52%), with intense gadolinium uptake and a fibrous component was the most frequent phenotype described. Optic nerve signal abnormalities were observed in 47% of cases. Two patients had bilateral homogeneous extraocular muscle enlargement suggestive of a myositis-like involvement of ECD-ROD. None had isolated dacryoadenitis but in 17 eyes dacryadenitis was described in association with other types of orbital lesions. Only seven patients (15%) had normal brain MRI findings. ECD-associated paranasal sinus involvement and post-pituitary involvement were detected in 56% and 53% of patients, respectively. A decrease/disappearance of the lesions was observed in 17/24 (71%) of the patients undergoing late (>12 months) follow-ups. Interestingly, ECD-ROD only rarely (7/45; 16%) revealed the disease, with exophthalmos being the most frequently identified feature in this subgroup (3/45; 6%). Even though ECD-ROD can be clinically silent, it comprises a broad array of lesions often resulting in optic nerve signal abnormalities, the functional outcome of which remains to be established. ECD-ROD should thus be assessed initially and subsequently monitored by orbital MRI and ophthalmological follow-up.

Introduction

Erdheim-Chester disease (ECD) is a rare, L-group histiocytosis¹ encompassing various pathophysiological processes and diverse clinical manifestations originating from the xanthomatous or xanthogranulomatous infiltration of tissues by foamy histiocytes, “lipid-laden” macrophages, or histiocytes, with the infiltrate surrounded by fibrosis.² It commonly affects the long bones (96-99%),²⁻⁴ and is frequently characterized by bilateral symmetric long-bone osteosclerosis.^{2,5-7} About half the patients present with extraskeletal manifestations, including orbital infiltration in about 30% of cases.⁸ Intraorbital infiltration, sometimes described as “intraorbital masses”, has been reported in

association with clinical exophthalmos in ECD patients.⁹⁻¹⁴ ECD-related orbital disease (ECD-ROD) may have imaging features in common with other causes of orbital inflammation, such as immunoglobulin G4-related orbital disease (IgG4-ROD), lymphoproliferative disease, or granulomatosis with polyangiitis, particularly if there is associated lacrimal gland involvement (dacryoadenitis). There is no published systematic description of a substantial series of patients with ECD-ROD, and no follow-up data are currently available. Our aim here was to characterize the orbital involvement in ECD by retrospectively reviewing orbital magnetic resonance imaging (MRI) findings. We also evaluated the available clinical and radiological follow-up data.

Methods

Study design

This retrospective study analyzing patients' medical records and imaging data was approved (n. 20210810160633) by the ethics committee of our institution (Pitié-Salpêtrière Hospital, Paris). It was conducted in accordance with the Declaration of Helsinki.

Population

Patients with a histologically proven diagnosis of ECD referred to our French tertiary center between 1996 and 2020 were enrolled in the study. The inclusion criteria were: (i) patient over 18 years of age; (ii) definitive diagnosis of ECD established on the basis of the consensus criteria;¹⁵ and (iii) available brain and orbital MRI. Patients with mixed histiocytosis (ECD and Langerhans cell histiocytosis/Rosai-Dorfman disease) were excluded.

Magnetic resonance imaging protocol

Orbital MRI included 3 or 1.5 Tesla images with at least T2-weighted (T2W) coronal and T1-weighted (T1W) spin-echo fat-saturated, gadolinium-enhanced sequences covering the entire orbit and the visual pathways, including the optic chiasm. Brain MRI included at least T2W- and diffusion-weighted imaging axial, three-dimensional or axial T2 fluid-attenuated inversion recovery (FLAIR) sequences.

Imaging analysis

The imaging data were collected and retrospectively reviewed by two neuroradiologists (YG and NS) with 5 and 7 years of experience in neuroradiology. Differences in assessment were settled by consensus with the third reader (DG) with 20 years of experience. Only the patients with positive identification of orbital lesions were included in the final imaging analysis. The readers assessed the following characteristics of each orbital lesion: (i) its lateral location, defined as left, right or bilateral; (ii) its location within orbital regions, as follows: adjacent to the globe, intraconal or extraconal orbital fat involvement, extraocular muscle, lacrimal gland; (iii) its main signal on T2W imaging, defined as hypointense, isointense or hyperintense, relative to the signal for healthy oculomotor muscles, the temporal muscles; (iv) its enhancement after contrast injection, relative to that of healthy extraocular muscles, classified as absent, moderate if weaker than that of healthy extraocular muscles, or major if at least as strong as that of healthy oculomotor muscles; (v) its extension to the cavernous sinus, foramen ovale or foramen rotundum; (vi) exophthalmos: defined as the posterior third of the orbital globe lying in front of the external bicanthal line;^{16,17} (vii) enophthalmos: defined as half the orbital globe lying behind the external bicanthal line; and (viii)

optic nerve T2 signal abnormality and optic nerve sheath enlargement.

The following information was collected from the brain MRI sequences: (i) the presence of thickening of the pituitary stem and/or a loss of spontaneous T1W hyperintensity of the posterior pituitary gland and infundibular stalk abnormalities; (ii) pachymeningeal and leptomenigeal involvement; (iii) intra-axial mass; (iv) high T2 FLAIR signal intensity within the dentate nuclei; (v) ischemic sequelae; and (vi) cortico-subcortical atrophy.

The presence of paranasal sinus involvement suggestive of ECD was also assessed. All of the available follow-up MRI scans were analyzed.

Clinical data, including age at the time of orbital MRI, sex, and BRAF status, were collected. Available visual acuity test results and the existence of associated cardiac damage or kidney damage were also assessed.

Statistical analysis

Age is expressed as the mean and standard deviation (SD). Categorical variables are expressed as counts and percentages. Comparisons between categorical variables were performed with the Fisher exact test and the χ^2 test, for univariate analysis. We considered *P* values <0.05 to be statistically significant. SPSS software was used for the analyses.

Results

Demographic data

In total, 304 patients with suspected ECD were referred to the internal medicine department of our hospital between January 1996 and July 2020. We excluded 62 (20%) of these patients due to mixed histiocytosis or because the diagnosis of ECD was not proven according to predefined and accepted criteria.^{2,15} The 137 brain MRI scans for the remaining patients included specific, orbital sequences, and 45 (33%) of these MRI revealed orbital abnormalities. The selection of participants is illustrated in Figure 1. The patients with orbital MRI abnormalities were mainly men (78%), with a mean age (\pm SD) of 60 (\pm 11.3) years. BRAF status was obtained for 122 of the 137 patients with proven ECD disease. A BRAF mutation was detected in 32 of the 80 (40%) without orbital abnormalities, and in 11 of the 42 (26%) patients with ECD-ROD (*P*=0.188, χ^2 test).

Orbital magnetic resonance imaging data

The initial MRI scans of 45 patients (83 affected eyes) were analyzed. Bilateral lesions were detected in 38 (84%) patients, and 25 (55%) patients had symmetric orbital involvement. Orbital fat infiltration was observed in 88% of cases, whereas the intraconal fat surrounding the optic nerve

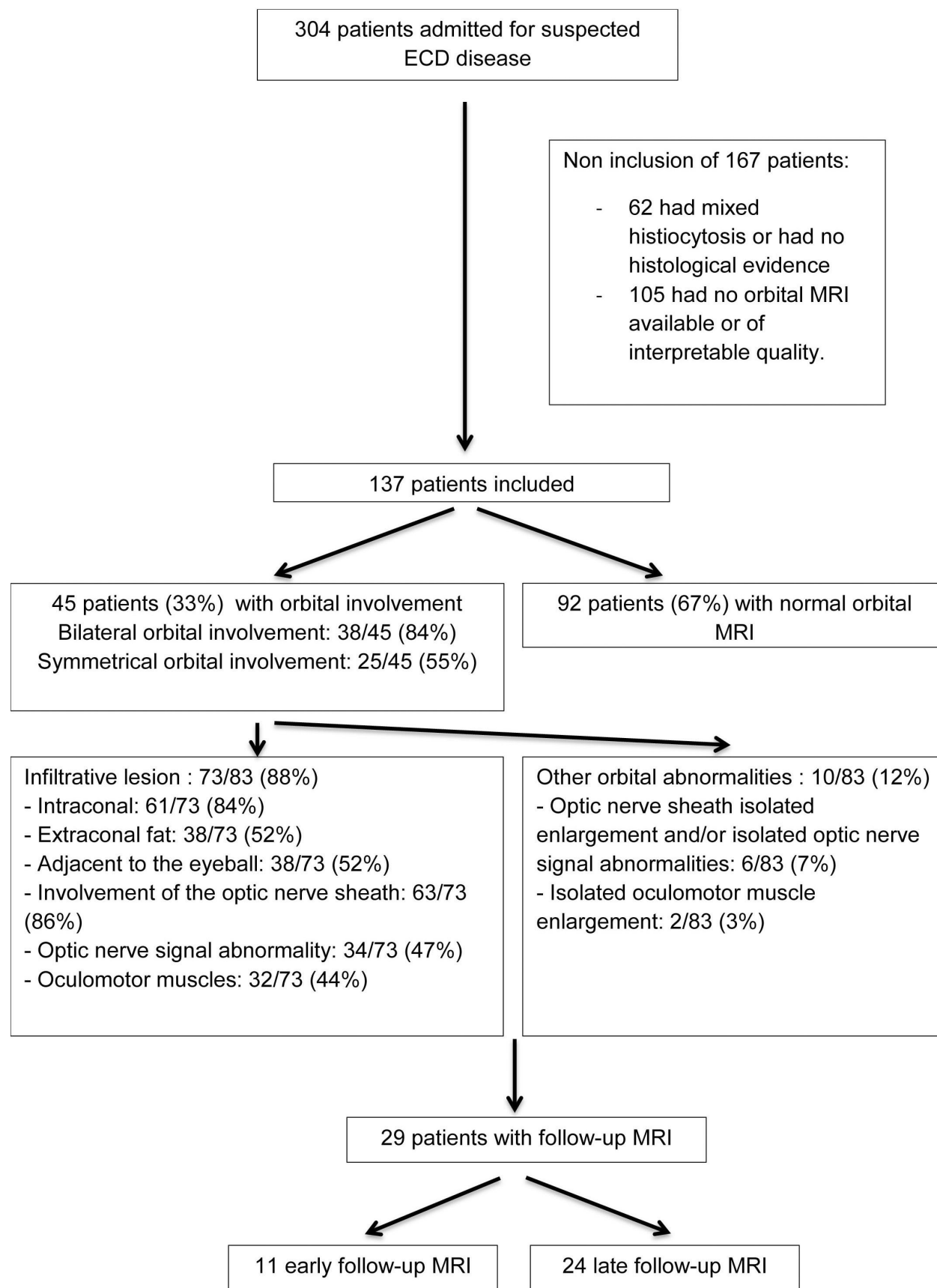


Figure 1. Flow-chart of the patients' inclusion and analysis. ECD: Erdheim-Chester disease; MRI: magnetic resonance imaging.

sheath was involved in 84% of cases. This involvement was anterior, adjacent to the eyeball, resulting in radiological images resembling “hairy globes” in 52% of cases. It resulted in optic nerve signal abnormalities in 47% of cases (Figure 2). For orbital infiltration, it was possible to assess the intensity of the T2W signal on MRI for only 67 affected eyes, due to significant movement artifacts. In most cases, the infiltration presented a hypointense T2W signal reflecting a fibrous component. We were able to analyze the gadolinium uptake of the infiltration in 69 affected eyes. The vast majority (90%) of lesions presented intense gadolinium

enhancement, with only 10% having weaker enhancement than for the temporal muscle. Interestingly, 7% of affected eyes displayed isolated bilateral optic nerve sheath enlargement and/or isolated optic nerve signal abnormalities. Two patients had homogeneous bilateral extraocular muscle enlargement (Figure 3). Both these patients tested negative for Graves' disease and neither was on interferon treatment. None of the patients had isolated dacryoadenitis. Only 31% of affected eyes presented exophthalmos, and 10% presented enophthalmos.

Orbital involvement is summarized in Table 1.

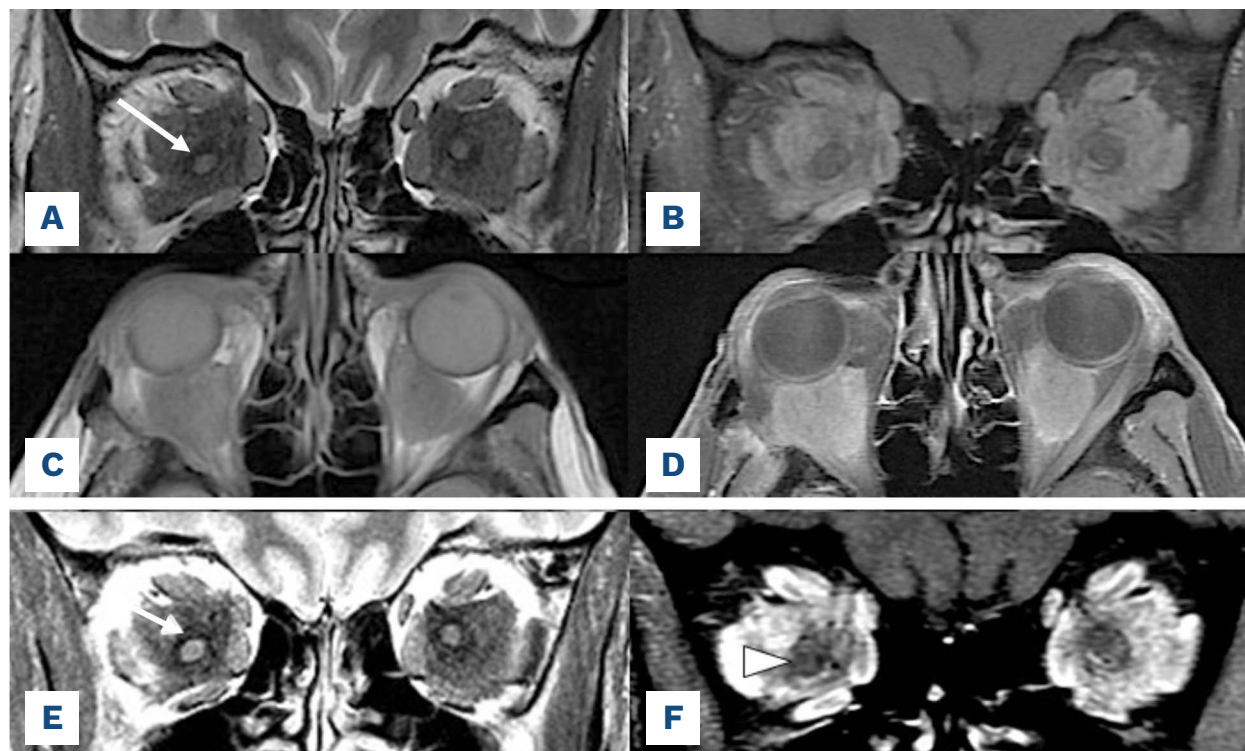


Figure 2. Orbital fat infiltration in two patients. (A-F) Magnetic resonance images. T2-weighted (A), T1-weighted with (B, D) and without (C) gadolinium enhancement sequences showing bilateral, anterior intraconal fat infiltration resulting in the signal abnormalities of the optic nerve (A, arrow). (E,F) Another patient with two layers of intraconal fat infiltration: the internal layer being hypointense on the T2-weighted image (E, arrow) and less enhanced on the T1-weighted sequence (F, arrowhead) than the peripheral one.

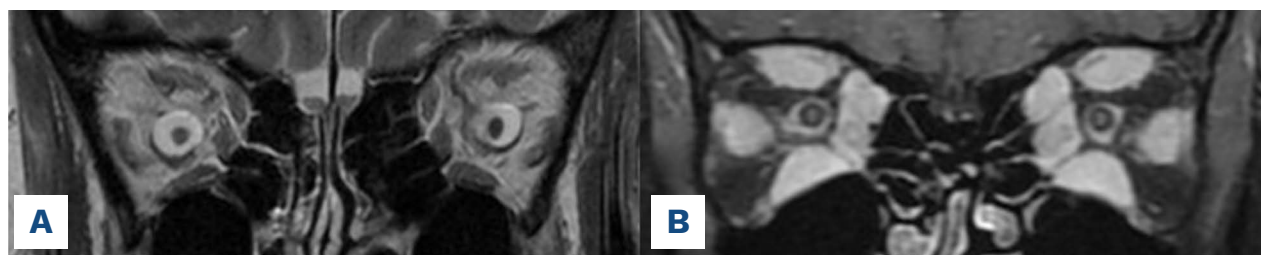


Figure 3. Other orbital abnormalities. (A) T2-weighted sequence showing an isolated bilateral optic nerve sheath enlargement. (B) T1-weighted fat saturated gadolinium enhanced image from a patient with bilateral homogeneous extraocular muscle enlargement.

Brain magnetic resonance imaging data

Out of 45 patients with orbital lesions only seven (15%) had normal brain MRI results. Paranasal sinus involvement (56%) and the loss of the T1W bright spot in the posterior pituitary lobe (53%) were the most frequent extraorbital findings. Cortico-subcortical atrophy was observed in 20 of 45 (45%) patients. The extraorbital lesions are summarized in Table 2. The brain MRI findings of the patients included before 2010 were reported by Drier *et al.*⁸

There was no significant statistical link between the presence of orbital, encephalic, and paranasal sinus lesions. For the 45 patients with orbital abnormalities, we found no significant associations with the involvement of other organs. No significant statistical link was detected between “hairy-globe” infiltration and the “hairy-kidney” sign ($P=0.5$). One of the three patients with isolated optic nerve hyperintensity had a history of glaucoma, whereas the other two had undergone no ophthalmological monitoring.

Follow-up magnetic resonance imaging data

Twenty-nine patients underwent at least one follow-up

MRI scan. Eleven patients underwent MRI at a check-up visit within 1 year (early follow-up), and 24/45 had longitudinal follow-up data for more than a year (late follow-up). Follow-up lasted a mean of 55 months and a median of 33.5 months (range, 7-238 months). Infiltration remained stable on the early follow-up MRI scans for all but one of the 11 patients with such scans available. Late follow-up MRI scans were performed for 24 patients (among whom 12 were treated with interferon- α , 5 with a BRAF inhibitor, 1 with dual therapy (BRAF + MEK inhibitor), 2 with remicade, 1 with tocilizumab, and 1 with anakinra). In 17 (71%) of the 24 patients the lesions decreased in size or disappeared. It should be noted that lesions decreased in two patients who were off therapy (Figure 4). For all these patients, we observed a decrease in the intensity of gadolinium uptake followed by a decrease in lesion volume. Two of the seven patients displaying no significant modification had an isolated enlargement of the optic nerve sheath. Four of the five remaining patients with infiltrative lesions had an initial hypointense signal lesion on the T2W sequence relative

to the intensity of the signal from temporal muscles, suggesting a mostly fibrous component.

We were able to collect visual acuity data for 26/45 patients. Sixteen (61%) had a visual acuity of 10/10. Three of the 45 patients (11%) had a visual acuity $\leq 5/10$, and all three had anterior “hairy-globe” lesions. Interestingly, orbital involvement was rarely (7/45; 16%) identified as the sign revealing the disease, and clinical exophthalmos was the most frequent form of optical involvement detected (3/45; 6%).

Discussion

This is, to the best of our knowledge, the largest study to date of patients with ECD-ROD. It is also the only study providing follow-up analysis of the orbital imaging. As such, it provided sufficient data for a rich topographical and semiological description. In this series of 137 patients,

Table 1. Results of orbital magnetic resonance imaging analysis.

Orbital lesions (N=45 patients)	N (%)
Bilateral orbital involvement	38/45 (84)
Symmetric orbital involvement	25/45 (55)
Infiltrative lesions (n=83 AE)	73/83 (88)
Infiltration morphology/location analysis	
Pre-orbital fat	3/73 (4)
Adjacent to the eyeball	38/73 (52)
Involvement of the optic nerve sheath	63/73 (86)
Intraconal fat	61/73 (84)
Extraconal fat	38/73 (52)
OMM	32/73 (44)
Lacrimal gland	18/73 (25)
Orbital apex	42/73 (58)
Infiltration signal analysis	
T2 signal \leq TM	51/67 (76)
T2 signal \leq healthy OMM	41/67 (61)
Major enhancement	62/69 (90)
Moderate enhancement	7/69 (10)
Optic nerve signal abnormality	34/73 (47)
Extraorbital involvement (cavernous sinus/ foramen ovale/ foramen rotundum)	7/73 (10)
Other orbital abnormalities (n=83 AE)	10/83 (12)
Isolated optic nerve sheath enlargement and/or isolated optic nerve signal abnormalities	6/83 (7)
Extraorbital muscle enlargement	4/83 (5)
Isolated lacrimal gland enlargement	0/83 (0)
Exophthalmos	26/83 (31)
Enophthalmos	8/83 (10)

AE: affected eyes; OMM: oculomotor muscles; TM: temporal muscles.

orbital MRI results were abnormal for 45 (33%) patients. The previously reported intraconal, anterior “hairy globe-like” lesions¹⁸⁻²² were the most frequent type in patients with ECD-ROD, but unilateral orbital abnormalities were not exceptional (16%) (Figure 5). Four affected eyes presented homogeneous extraocular muscle enlargement with no significant intraorbital fat infiltration. This myositis-like pattern of ECD-ROD has not previously been reported in ECD-ROD. This new feature is of particular importance for the differential diagnosis of Graves’ disease-associated orbitopathy or idiopathic orbital myositis-related inflammation.²³ Only 31% of the patients had exophthalmos evident on radiological examination, and ophthalmological symptoms revealed the disease in only 16% of cases. However, a large proportion of patients (47% of affected eyes with intraorbital fat infiltration) presented optic nerve signal abnormalities. Given the scarcity of residual visual acuity data and the lack of systematic monitoring of the visual field or retinal thickness, both of which are expected to be modified by chronic extrinsic compression, no conclusions can yet be drawn about the clinical implications of this finding.²⁴⁻²⁶

Head MRI results were frequently abnormal in the patients with orbital lesions (85%). Consistent with the findings of previous studies, associated lesions most frequently detected were paranasal sinus and pituitary lobe abnormalities.⁸

Late follow-up MRI revealed a remarkable decrease in the size of orbital infiltrative lesions or the total disappearance of these lesions. Gadolinium enhancement, reflecting the intensity of inflammation, was the first sign to disappear during follow-up.

Case reports and very small series of patients have resulted in descriptions of ophthalmological symptoms such

Table 2. Associated brain and sinus involvement.

Cortico-subcortical atrophy, N (%)	20/45 (44)
Ischemic sequelae, N (%)	4/45 (8)
Intra-axial mass, N (%)	2/45 (4)
High T2 FLAIR signal intensity in the dentate nucleus area, N (%)	12/45 (27)
Diffuse pachymeningeal thickening, N (%)	9/45 (20)
Diffuse leptomenigeal thickening, N (%)	1/45 (2)
Infundibular stalk abnormalities, N (%)	6/45 (13)
Absence of T1 bright spot in the posterior pituitary lobe, N (%)	23/43 (53)
Sinus involvement, N (%)	25/45 (56)

FLAIR: fluid-attenuated inversion recovery.

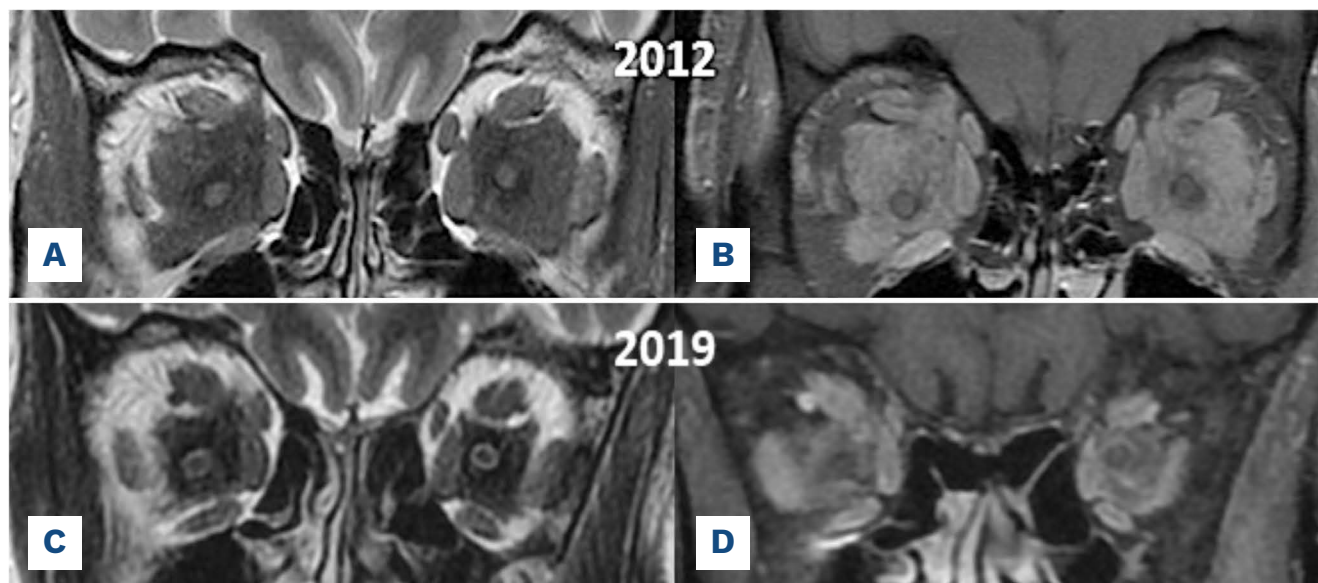


Figure 4. Erdheim-Chester disease-related orbital disease with a follow-up. T2-weighted (A, C) and T1-weighted fat saturated gadolinium enhanced (B, D) initial (A, B) and follow-up magnetic resonance images (C, D), demonstrating an important decrease in lesion size as well as a reduction in gadolinium uptake.

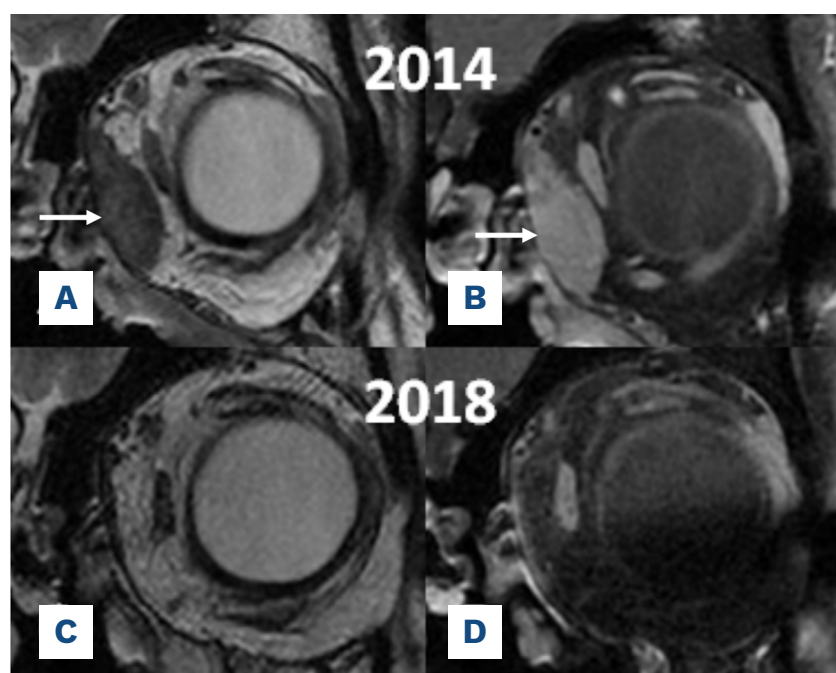


Figure 5. Unilateral extraconal lesion. T2-weighted (A, C) and T1-weighted fat saturated, gadolinium enhanced (B, D) magnetic resonance images showing a well-delimited lesion within extraconal fat (A, B, arrow) and its disappearance on the follow-up images (C, D).

as reduced visual acuity or exophthalmos associated with ECD-ROD, which is often the first clinical manifestation of the disease.^{10,11,22,27,28} In our study, ophthalmological symptoms (exophthalmos) helped to reveal the disease in only a small proportion of cases. When available, the visual acuity seemed to be generally well preserved (89% had a visual acuity $\geq 6/10$), but no data were available concerning retinal nerve fiber layer thickness/visual field. No isolated lacrimal gland lesions were observed in our series. Furthermore, the extension of lesions towards the cavernous sinus/foramen rotundum was very rare (10% of the infiltrative lesions). This feature may be of use for distinguishing between ECD-ROD and its principal differential diagnoses, such as IgG4-ROD and sarcoidosis. Of note, almost every orbital structure may be involved in IgG4-ROD, lacrimal gland involvement being the most frequent (up to 53-87.7%).²⁹⁻³¹ Orbital involvement may be isolated.^{30,32} Perineural spread along the V1, V2 (into the foramen ro-

tundum) and especially V3 branches (into the foramen ovale) is a specific feature of IgG4-ROD.³² The most common orbital features in neurosarcoidosis include uveitis,³³ lacrimal gland involvement (42% and 63%)^{34,35} and retrobulbar optic neuritis (63%).

The most recent consensus recommendations¹⁵ indicate the performance of brain MRI with gadolinium injection during initial diagnostic investigations. However, these recommendations do not stress the importance of including specific orbital sequences. The results of our study demonstrate the difficulty of diagnosing ECD-ROD and the need for systematic orbital MRI sequences to be included in the initial assessment and follow-up of ECD-associated organ involvement.

The retrospective design of this study was one of its limitations. Furthermore, the rarity of the disease necessitated the collection of data for patients seen over a period of 24 years, to ensure the inclusion of sufficient numbers

of patients. These data were, inevitably, incomplete, and the quality of the orbital MRI scans available was highly variable, in terms of both the sequences performed and their resolution. Visual acuity data were available for only 56% of patients, and no data on the visual field or the thickness of the retinal nerve fiber layer were available for a substantial number of patients.

In conclusion, ECD-ROD corresponds to an array of lesions, mostly silent, but often resulting in optic nerve signal abnormalities. The initial assessment and subsequent monitoring of ECD-ROD by orbital MRI and ophthalmological follow-up is therefore essential to prevent possible functional handicaps, such as visual field limitation.

Disclosures

No conflicts of interest to disclose.

References

- Emile J-F, Abla O, Fraitag S, et al. Revised classification of histiocytoses and neoplasms of the macrophage-dendritic cell lineages. *Blood*. 2016;127(22):2672-2681.
- Haroche J, Arnaud L, Cohen-Aubart F, et al. Erdheim-Chester disease. *Curr Rheumatol Rep*. 2014;16(4):412.
- Mazor RD, Manevich-Mazor M, Shoenfeld Y. Erdheim-Chester disease: a comprehensive review of the literature. *Orphanet J Rare Dis*. 2013;8:137.
- Arnaud L, Hervier B, Néel A, et al. CNS involvement and treatment with interferon- α are independent prognostic factors in Erdheim-Chester disease: a multicenter survival analysis of 53 patients. *Blood*. 2011;117(10):2778-2782.
- Dion E, Graef C, Miquel A, et al. Bone involvement in Erdheim-Chester disease: imaging findings including periostitis and partial epiphyseal involvement. *Radiology*. 2006;238(2):632-639.
- Estrada-Veras JI, O'Brien KJ, Boyd LC, et al. The clinical spectrum of Erdheim-Chester disease: an observational cohort study. *Blood Adv*. 2017;1(6):357-366.
- Veyssier-Belot C, Cacoub P, Caparros-Lefebvre D, et al. Erdheim-Chester disease. Clinical and radiologic characteristics of 59 cases. *Medicine (Baltimore)*. 1996;75(3):157-169.
- Drier A, Haroche J, Savatovsky J, et al. Cerebral, facial, and orbital involvement in Erdheim-Chester disease: CT and MR imaging findings. *Radiology*. 2010;255(2):586-594.
- Alper MG, Zimmerman LE, Piana FG. Orbital manifestations of Erdheim-Chester disease. *Trans Am Ophthalmol Soc*. 1983;81:64-85.
- Broccoli A, Stefoni V, Faccioli L, et al. Bilateral orbital Erdheim-Chester disease treated with 12 weekly administrations of VNCOP-B chemotherapy: a case report and a review of literature. *Rheumatol Int*. 2012;32(7):2209-2213.
- Gilles M, Alberti N, Seguy C, et al. [An ophthalmologic diagnostic error leading to a rare systemic diagnosis: Erdheim-Chester disease]. *J Fr Ophtalmol*. 2014;37(5):377-380.
- Mamlouk MD, Aboian MS, Glastonbury CM. Case 245: Erdheim-Chester disease. *Radiology*. 2017;284(3):910-917.
- de Abreu MR, Chung CB, Biswal S, et al. Erdheim-Chester disease: MR imaging, anatomic, and histopathologic correlation of orbital involvement. *AJNR Am J Neuroradiol*. 2004;25(4):627-630.
- Sheidow TG, Nicolle DA, Heathcote JG. Erdheim-Chester disease: two cases of orbital involvement. *Eye (Lond)*. 2000;14(Pt 4):606-612.
- Goyal G, Heaney ML, Collin M, et al. Erdheim-Chester disease: consensus recommendations for evaluation, diagnosis, and treatment in the molecular era. *Blood*. 2020;135(22):1929-1945.
- Héran F, Lafitte F. Chapitre 4 - Pathologie orbitopalpebrale: Exophtalmie. In: Héran F, Lafitte F, eds. *Imagerie en Ophtalmologie pour les Radiologues*. Elsevier Masson; 2018:81-153.e30.
- Fang ZJ, Zhang JY, He WM. CT features of exophthalmos in Chinese subjects with thyroid-associated ophthalmopathy. *Int J Ophthalmol*. 2013;6(2):146-149.
- Grumbine FL, Aderman C, Vagefi MR, et al. Orbital MRI pre- and post-venlafaxine therapy for Erdheim-Chester disease. *Ophthalmic Plast Reconstr Surg*. 2015;31(6):e169.
- Pineles SL, Liu GT, Acebes X, et al. Presence of Erdheim-Chester disease and Langerhans cell histiocytosis in the same patient: a report of 2 cases. *J Neuroophthalmol*. 2011;31(3):217-223.
- Lau WW, Chan E, Chan CW. Orbital involvement in Erdheim-Chester disease. *Hong Kong Med J*. 2007;13(3):238-240.
- Perić P, Antić B, Knezević-Usaj S, et al. Successful treatment with cladribine of Erdheim-Chester disease with orbital and central nervous system involvement developing after treatment of Langerhans cell histiocytosis. *Vojnosanit Pregl*. 2016;73(1):83-87.
- Abdellateef EE, Abdelhai AR, Gawish HH, et al. The first reported case of Erdheim-Chester disease in Egypt with bilateral exophthalmos, loss of vision, and multi-organ involvement in a young woman. *Am J Case Rep*. 2016;17:360-370.
- Mombaerts I, Bilyk JR, Rose GE, et al. Consensus on diagnostic criteria of idiopathic orbital inflammation using a modified Delphi approach. *JAMA Ophthalmol*. 2017;135(7):769-776.
- Rosiene J, Liu X, Imielinska C, et al. Structure-function relationships in the human visual system using DTI, fMRI and visual field testing: pre- and post-operative assessments in patients with anterior visual pathway compression. *Stud Health Technol Inform*. 2006;119:464-466.
- Ryu WHA, Starreveld Y, Burton JM, et al. The utility of magnetic resonance imaging in assessing patients with pituitary tumors

- compressing the anterior visual pathway. *J Neuroophthalmol.* 2017;37(3):230-238.
26. Danesh-Meyer HV, Yoon JJ, Lawlor M, et al. Visual loss and recovery in chiasmal compression. *Prog Retin Eye Res.* 2019;73:100765.
27. Pichi F. Choroidal mass as the first presentation of Erdheim-Chester disease. *Am J Ophthalmol Case Rep.* 2019;16:100539.
28. Valmaggia C, Neuweiler J, Fretz C, et al. A case of Erdheim-Chester disease with orbital involvement. *Arch Ophthalmol.* 1997;115(11):1467-1468.
29. Shor N, Sené T, Zuber J, et al. Discriminating between IgG4-related orbital disease and other causes of orbital inflammation with intra voxel incoherent motion (IVIM) MR imaging at 3T. *Diagn Interv Imaging.* 2021;102(12):727-734.
30. Tiegs-Heiden CA, Eckel LJ, Hunt CH, et al. Immunoglobulin G4-related disease of the orbit: imaging features in 27 patients. *AJNR Am J Neuroradiol.* 2014;35(7):1393-1397.
31. Sogabe Y, Ohshima K, Azumi A, et al. Location and frequency of lesions in patients with IgG4-related ophthalmic diseases. *Graefes Arch Clin Exp Ophthalmol.* 2014;252(3):531-538.
32. Ben Soussan J, Deschamps R, Sadik JC, et al. Infraorbital nerve involvement on magnetic resonance imaging in European patients with IgG4-related ophthalmic disease: a specific sign. *Eur Radiol.* 2017;27(4):1335-1343.
33. Lutt JR, Lim LL, Phal PM, et al. Orbital inflammatory disease. *Semin Arthritis Rheum.* 2008;37(4):207-222.
34. Prabhakaran VC, Saeed P, Esmali B, et al. Orbital and adnexal sarcoidosis. *Arch Ophthalmol.* 2007;125(12):1657-1662.
35. Demirci H, Christianson MD. Orbital and adnexal involvement in sarcoidosis: analysis of clinical features and systemic disease in 30 cases. *Am J Ophthalmol.* 2011;151(6):1074-1080.e1.
36. Leclercq M, Sené T, Chapelon-Abric C, et al. Prognosis factors and outcomes of neuro-ophthalmologic sarcoidosis. *Ocul Immunol Inflamm.* 2020;9:1-8.